Mirror at the edge of the universe: Reflections on an accelerated boundary correspondence with de Sitter cosmology

Michael R. R. Good,[1,2,*] Abay Zhakenuly,[1,†] and Eric V. Linder[2,3,‡]

[1]*Physics Department, Nazarbayev University, Nur-Sultan 010000, Kazakhstan*
[2]*Energetic Cosmos Laboratory, Nazarbayev University, Nur-Sultan 010000, Kazakhstan*
[3]*Berkeley Center for Cosmological Physics & Berkeley Lab, University of California, Berkeley, 94720 California, USA*

(Received 16 May 2020; accepted 10 August 2020; published 28 August 2020)

An accelerated boundary correspondence (ABC) is solved for the de Sitter moving mirror cosmology. The beta Bogoliubov coefficients reveal the particle spectrum is a Planck distribution with temperature inversely proportional to horizon radius. The quantum stress tensor indicates a constant emission of energy flux consistent with eternal equilibrium, while the total energy carried by the particles remains finite. The curved spacetime transformation to flat spacetime with an accelerated boundary is illustrated, and also shown for anti-de Sitter (AdS) spacetime.

DOI: 10.1103/PhysRevD.102.045020

I. INTRODUCTION

Einstein used a moving mirror in his seminal 1905 work to derive the relativistic Doppler effect. Schrödinger, in 1939, determined that our expanding universe results in particle creation [1]. A beautiful union of these seemingly disparate ideas occurred in the 1970s when it was calculated that an accelerating mirror [2] could also produce its own radiation, in close analog [3] to black hole particle creation [4].

Understanding the thermodynamics and quantum particle production of de Sitter space [5–7] is well motivated both mathematically, since it is the maximally symmetric solution of Einstein's equations with a positive cosmological constant, and physically, since during the early universe, $t \lesssim 10^{-32}$ s, inflation is approximately de Sitter [8] and with current cosmic acceleration the cosmos may be headed for a future de Sitter state.

The static coordinate metric of de Sitter is given by

$$ds^2 = -\left(1 - \frac{r^2}{L^2}\right)dt^2 + \left(1 - \frac{r^2}{L^2}\right)^{-1} dr^2 + r^2 d\Omega, \quad (1)$$

with $d\Omega \equiv d\theta^2 + \sin^2\theta\, d\phi^2$. We transform de Sitter space, with its horizon at $r = L$, to the analogous moving mirror model [9,10] trajectory, with the accelerating boundary playing the role of the origin of coordinates, to study quantum particle production, i.e., the dynamical Casimir effect (see e.g., recent experimental proposals [11,12]).

Moving mirrors have proved themselves very useful in different contexts, in particular as $(1+1)$-dimensional toy models because they are much simpler than the realistic $(3+1)$-dimensional systems they imitate and therefore may admit exact and relatively simple analytical solutions, which often provide some insight into the real effects. We utilize this advantage of the moving mirror model to investigate thermal particle production for a particular trajectory that is associated with de Sitter spacetime.

In Sec. II we derive the relation between the de Sitter metric and the de Sitter moving mirror through mapping in $(1+1)$-dimensional accelerated coordinates and matching in $(3+1)$-dimensional curved spacetime null sphere expansion. Section III computes the quantum particle spectrum and compares it to the late-time Schwarzschild mirror solution (the eternal black hole spectrum of the Carlitz-Willey mirror). We extend the mapping to anti-de Sitter (AdS) space in Sec. IV.

II. FROM DE SITTER METRIC TO ACCELERATION

Our aim is to explicitly solve for the spectrum of the thermal moving mirror in flat spacetime which is most closely related to the curved spacetime of de Sitter. In explicit form, the beta Bogobliubov coefficients for particle production of a massless scalar field in the static coordinate metric of de Sitter spacetime, to our best knowledge, have not previously been derived.

The spherically symmetric, static metric

$$\mathrm{d}s^2 = -f(r)\mathrm{d}t^2 + f(r)^{-1}\mathrm{d}r^2 + r^2\mathrm{d}\Omega \quad (2)$$

*michael.good@nu.edu.kz
†abay.zhakenuly@nu.edu.kz
‡evlinder@lbl.gov

corresponds to the inside static metric of the de Sitter expansion system for $f(r) \equiv f_L$ with

$$f_L = 1 - \frac{r^2}{L^2}. \tag{3}$$

While it looks similar to a black hole spacetime, here the observer lives in the inside, $0 < r < L$, with a cosmological horizon at $r = L$. The temperature seen by an inertial observer in de Sitter spacetime is

$$T = \frac{1}{2\pi L}, \tag{4}$$

(see Appendix A for a derivation which does not solve for the beta coefficients directly). We set $G = \hbar = c = 1$.

A. Relating 3 + 1 spacetime and 1 + 1 mirror

In [13] Davies exploited the conformal invariance of the $(1 + 1)$-dimensional massless wave equation and globally identified the origin of coordinates with a rapidly receding mirror, recognizing the same behavior for the center of coordinates of a $(3 + 1)$-dimensional spherically symmetric star which acts mathematically as a Dirichlet boundary accelerating away from outside observers as the star collapses to a black hole. The boundary "moves" as a consequence of the Minkowski-to-Rindler coordinate transformation. See Fulling-Wilson [14] which relates the coordinate procedure to the moving mirror model in Rindler coordinates.

On the other hand, there is a different physical system in [3,15–17] where there is a joining between two spacetimes to model black hole collapse. In that model there is a suturing of a curved region to a flat region along some curve. The mathematics is very similar and the matching procedure in these works is purposefully applied to model a collapsing shell of matter forming a black hole. In seminal work [10], Fulling and Davies also considered a black hole, but only of the eternal Kruskal variety with no incoming matter.

In this paper, we find and confirm the form of the moving mirror by treating the de Sitter scenario in both systems (mapping and matching). As an accelerated frame mapping, akin to Davies [13], done in full generality for any conformal mapping by Sanchez [18,19], there is a Minkowski-to-de Sitter transformation, $u(U)$ (that will function as the moving mirror), between inertial Minkowski coordinates (U, V) and accelerated de Sitter coordinates (u, v).

In the matching interpretation, the $u(U)$ is the matching condition of the $(3 + 1)$-dimensional curved spacetime system like the calculations in [3,15–17] that model dynamic collapse. In order to find the $u(U)$ condition that gives the relevant mirror trajectory of interest, the radial coordinate matching, $r = r^*$, is done over a light ray $v = v_0$. Once the matching $u(U)$ is found, the de Sitter moving mirror is read off as the identical function, but expressed in flat Minkowski spacetime as the retarded time function $f(v)$ with advanced time as the independent variable.

With the de Sitter moving mirror, $f(v)$, in hand, the focus of this paper will turn from the $(3 + 1)$-dimensional curved spacetime system [or the $(1 + 1)$-dimensional accelerated coordinate system] and exactly solve the $(1 + 1)$-dimensional massless scalar single moving mirror model in flat spacetime using Minkowski coordinates only. The connection to de Sitter space comes from solving for the mirror $f(v)$ from the $u(U)$ in the analogous $(1 + 1)$-dimensional accelerated coordinate mapping (Sec. II B) or the $(3 + 1)$-dimensional curved spacetime matching (Sec. II C). In the matching situation, the de Sitter metric is utilized rather than a black hole metric. In the mapping situation, the de Sitter coordinates are utilized rather than Rindler coordinates.

B. Mapping

Consider mapping from Minkowski coordinates, (U, V) to a "de Sitter" accelerated coordinate system, (u, v). We express the conformally flat spacetimes in $(1 + 1)$ dimensions as $ds^2 = -\mathrm{d}U\,\mathrm{d}V$, and $ds^2 = -f_L\,\mathrm{d}u\,\mathrm{d}v$, respectively. To find $u(U)$ we integrate,

$$\frac{\mathrm{d}u}{\mathrm{d}U} = \frac{1}{f_L}, \tag{5}$$

and obtain

$$u(U) = 2L \tanh^{-1} \frac{U - v}{2L}, \tag{6}$$

where we have substituted for r using $2r = V - U$ and set $V(v) = v$. To reduce to a moving mirror system of Fulling-Davies [9] the conformal factor must be a function of u alone, explicitly confirmed in Davies-Fulling-Unruh [3]. We therefore set $v = 0$ so

$$u(U) = 2L \tanh^{-1} \frac{U}{2L}, \tag{7}$$

which will have an analog in the following matching interpretation section where the matching is done over the null ray $v = v_0$, with the light sphere location set to zero, $v_0 = 0$. The general mapping of Sanchez [18,19] allows one to identify the appropriate moving mirror trajectory, $f(v)$ from the mapping function $u(U)$ of Eq. (7).

C. Matching

Now we qualitatively develop a dynamic-type model where one can envision the origin of the flat Minkowski spacetime as moving relative to the de Sitter curved spacetime observer. Matching to a flat region is done in

mathematical analogy to black hole collapse where the inside is flat. However, in this de Sitter case, it is the exterior that is flat because the observer resides inside de Sitter space. The crucial equation of interest is the correct matching condition $u(U)$, gleaned from the de Sitter tortoise coordinate. For a double null coordinate system (u, v), with $u = t - r^*$ and $v = t + r^*$, the appropriate tortoise coordinate [6] is

$$r^* = \int f_L^{-1} dr = \frac{L}{2} \ln \left| \frac{L + r}{L - r} \right| = L \tanh^{-1} \frac{r}{L}, \tag{8}$$

and one has the $(3 + 1)$-dimensional metric for the geometry describing the inside region $0 < r < L$,

$$\mathrm{d}s^2 = -f_L \, \mathrm{d}u \, \mathrm{d}v + r^2 \mathrm{d}\Omega. \tag{9}$$

We call (u, v) the interior coordinates. For a double null coordinate system (U, V) with $U = T - r$ and $V = T + r$, we have

$$\mathrm{d}s^2 = -\mathrm{d}U \, \mathrm{d}V + r^2 \mathrm{d}\Omega. \tag{10}$$

We call (U, V) the exterior coordinates. We aim to find the matching condition (see e.g., [3,15–17]), which will be the "trajectory" of $r = 0$, expressed in terms of the interior function $u(U)$ with exterior coordinate U. In the infinite past the spacetime is flat and there is no difference between the exterior and interior coordinates, allowing us to choose $V(v) = v$, as we did in the previous mapping subsection. Following [16], the mathematical procedure of setting $r = r^*$ over $v = v_0$ results in an implicit relationship over the gauge invariant coordinate radius,

$$r^* \left(r = \frac{v_0 - U}{2} \right) = \frac{v_0 - u}{2}, \tag{11}$$

which defines the area of a two-sphere at constant radius and time. Explicitly, using Eq. (8) we set

$$L \tanh^{-1} \frac{v_0 - U}{2L} = \frac{v_0 - u}{2}, \tag{12}$$

and rearrange, solving for $u(U)$:

$$u(U) = v_0 - 2L \tanh^{-1} \frac{v_0 - U}{2L}. \tag{13}$$

The matching of $r = r^*$ happens along a light sphere, v_0. Since we are simply after the radial trajectory of the origin, $u(U)$, which will function as the moving mirror, $f(v)$, there is no pressing need for a shell of matter on the null surface $v = v_0$ as in black hole collapse. Here $v_0 \pm 2L \equiv v_H$ because $u \to \pm\infty$ at $U = v_H$, and we obtain two horizons. Without loss of generality we can set $v_0 = 0$, which centers the system and simplifies the form of $u(U)$. The two horizons are at $v_H = \pm 2L$. The matching condition simplifies to

$$u(U) = 2L \tanh^{-1} \frac{U}{2L}, \tag{14}$$

which is the same as the mapping Eq. (7). It is at this point that our problem has effectively become $(1 + 1)$ dimensional. Further calculations along this line of inquiry give us only qualitative information about $(3 + 1)$-dimensional physics. However, quantitatively we can investigate the $(1 + 1)$-dimensional single moving mirror problem and look for analogous physics. For example, since de Sitter spacetime is thermal, we expect that the correct mirror choice will also be thermal. Interestingly, as a moving mirror, Eq. (14) is exactly all that is needed for understanding how the field modes become modified, resulting in particle creation in the simplified flat spacetime context of the moving mirror model. That is, Eq. (14) gives the boundary condition that defines the mode behavior.

In the curved spacetime system, the quantum field must be zero at $r = 0$, ensuring regularity of the modes, such that the origin acts like a moving mirror in the (U, V) coordinates. Since there is no field behind $r < 0$, the form of field modes can be determined, such that a $U \leftrightarrow v$ identification is made for the Doppler-shifted right movers of the moving mirror model. We are now ready to analyze the analog mirror trajectory, $f(v)$ from $u(U)$, as a known function of advanced time v.

D. Mirror

In the standard moving mirror formalism [20] we study the massless scalar field in $(1 + 1)$-dimensional Minkowski spacetime (following e.g., [21]). From Eq. (14) the de Sitter analog moving mirror trajectory is

$$f(v) = \frac{2}{\kappa} \tanh^{-1} \frac{\kappa v}{2}, \tag{15}$$

which is now a perfectly reflecting boundary in flat spacetime rather than the origin as a function of coordinates in curved de Sitter spacetime. Introduction of $\kappa \equiv L^{-1}$ is done to signal that we are now working in the moving mirror model with a background of flat spacetime, where κ is the acceleration parameter of the trajectory.

The horizons are $v_H = \pm 2/\kappa$, and so κv spans $-2 < \kappa v < +2$. The rapidity, in advanced time, $-2\eta(v) = \ln f'(v)$, is

$$\eta(v) = \frac{1}{2} \ln \left(1 - \frac{\kappa^2 v^2}{4} \right). \tag{16}$$

The rapidity asymptotes at $\kappa v = \pm 2$, i.e., the mirror approaches the speed of light at the horizons, $u \to \pm\infty$. The trajectory in spacetime coordinates is plotted as a

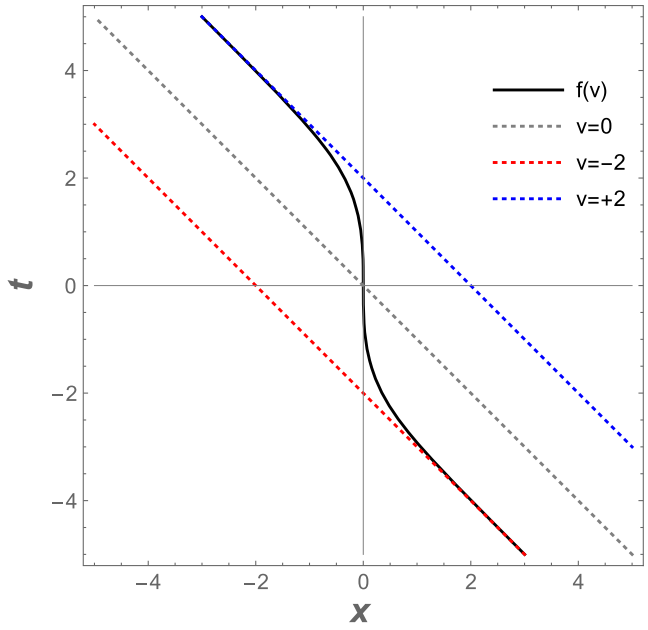

FIG. 1. Trajectories, Eq. (15), in a spacetime plot. The mirror is the thick black line. The horizons are at $\kappa v_H = \pm 2$ (blue and red dotted lines) and the $v = 0$ line is shown by the gray dotted line, where retarded time is $u = t - x$, and $v = t + x$ is advanced time.

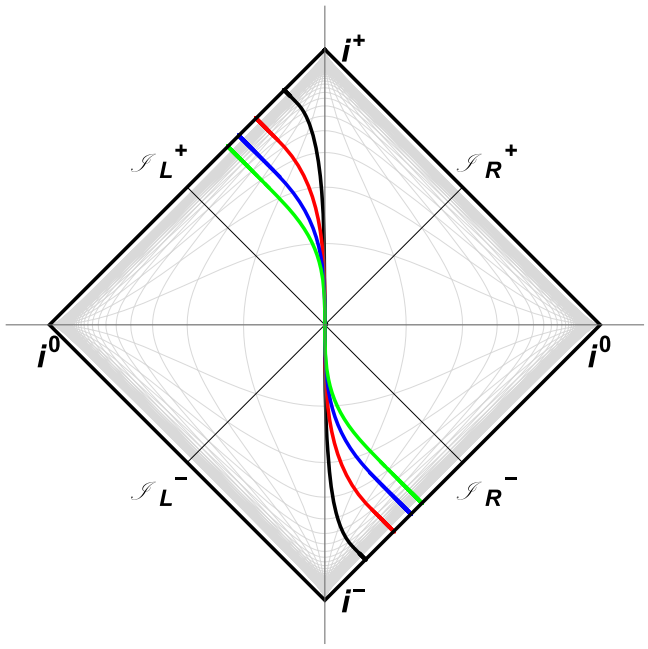

FIG. 2. The class of trajectories Eq. (15) in a Penrose conformal diagram. The colors correspond to different $\kappa = 1, 2, 3, 4$: black, red, blue, green, respectively. The trajectories extend all the way out to the null future and past surfaces.

spacetime plot in Fig. 1. A conformal diagram of the accelerated boundary is given in Fig. 2. (Note that x, defined by $u = t - x$, is the space coordinate in the mirror flat spacetime and is not restricted as $r > 0$; we choose $t = 0$, $x = 0$ as the "present." In some sense this is moot: the mirror is eternally thermal as we show so it does not matter if we restrict its trajectory to some range in space.)

The proper acceleration $\alpha = e^{\eta(v)}\eta'(v)$ is

$$\alpha(v) = -\frac{1}{2}\frac{\kappa^2 v}{\sqrt{4-\kappa^2 v^2}}, \tag{17}$$

where prime denotes derivative with respect to the argument. Note the acceleration is zero at $v = 0$, but approaches $\pm\infty$ near the horizons. The acceleration also takes on a simple form in terms of proper time, as discussed in Appendix B 1.

The double divergence in the advanced time acceleration Eq. (17) is arguably the main trait characterizing the de Sitter trajectory. As a result, the de Sitter mirror possesses a double asymptotic null horizon in contrast to the single horizons of the Schwarzschild mirror [22–24] and the recently calculated trajectory of the extreme Reissner-Nordström mirror [25]. Even the Reissner-Nordström mirror [26] (whose black hole has two horizons) has only one outer horizon relevant for its time-dependent particle production calculation. We will find the double horizons play an important role in the particle spectrum.

III. FLUX, SPECTRUM, AND PARTICLES

For the de Sitter mirror, we find that the energy flux is constant, eternally. The radiated energy flux as computed from the quantum stress tensor is the Schwarzian derivative of Eq. (15) [27],

$$F(v) = \frac{1}{24\pi}\{f(v), v\}f'(v)^{-2}, \tag{18}$$

where the Schwarzian brackets are defined as

$$\{f(v), v\} \equiv \frac{f'''}{f'} - \frac{3}{2}\left(\frac{f''}{f'}\right)^2, \tag{19}$$

which yields

$$F = \frac{\kappa^2}{48\pi}. \tag{20}$$

This result is indicative of thermal equilibrium and we next present the derivation of the accompanying Planck distribution.

The particle spectrum is given by the beta Bogoliubov coefficient, which can be found via [27]

$$\beta_{\omega\omega'} = -\frac{1}{4\pi\sqrt{\omega\omega'}}\int_{v_H^-}^{v_H^+} dv\, e^{-i\omega' v - i\omega f(v)}(\omega f'(v) - \omega'), \tag{21}$$

where ω and ω' are the frequencies of the outgoing and ingoing modes respectively. The result of the integration is

$$\beta_{\omega\omega'} = \frac{2\sqrt{\omega\omega'}}{\kappa^2 \sinh \pi\omega/\kappa} e^{-2i\omega'/\kappa} M(1 + i\omega/\kappa; 2; 4i\omega'/\kappa), \quad (22)$$

where $M := {}_1F_1$ the confluent hypergeometric function, i.e., the Kummer function of the first kind. The same betas [28,29] have been derived in the context of spacetime diamonds [30].

To obtain the particle spectrum, we complex conjugate,

$$N_{\omega\omega'} \equiv |\beta^{\rm dS}_{\omega\omega'}|^2, \quad (23)$$

giving the particle count per mode squared, plotted in Fig. 3. The spectrum N_ω is then

$$N_\omega = \int_0^\infty N_{\omega\omega'} d\omega', \quad (24)$$

plotted in Fig. 4, illustrating graphically a thermal Planck particle number spectrum. Multiplying by the energy and phase space factors gives the usual Planck blackbody energy spectrum.

Thermal behavior can also be seen analytically by the expectation value of the particle number, $\mathcal{N}_\omega$, via continuum normalization modes,

$$\mathcal{N}_\omega \equiv \int_0^{+\infty} d\omega' \beta_{\omega\omega'} \beta^*_{\omega_2\omega'} = \frac{\delta(\omega - \omega_2)}{e^{2\pi\omega/\kappa} - 1}. \quad (25)$$

We have used the textbook notation of [17], where the late-times Hawking case is done. As shown there, the delta

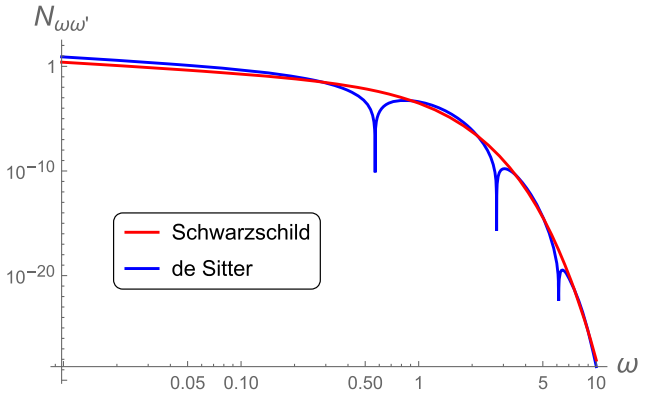

FIG. 3. The mode spectra $N_{\omega\omega'} \equiv |\beta_{\omega\omega'}|^2$, setting $\omega' = 1$ for illustration. The blue curve is the de Sitter case from Eqs. (22) and (23), while the red curve is the late time Schwarzschild result (or equivalent Carlitz-Willey mirror [31]) of Eq. (C16). A larger prefactor on the beta elevates the de Sitter spectra, offsetting the dips in frequency that are zeros in the mode spectrum due to Kummer's function, indicative of complete spectral absorption lines in the measure $|\beta_{\omega\omega'}|^2$. The zeros occur at $\omega = 0.57$, 2.74, 6.14, ad inf. The destructive interference, like in the double-slit experiment, could be between the double horizons, as field modes do not propagate freely asymptotically, i.e., $e^{i\omega v}$ has a boundary at $v = \pm v_H$.

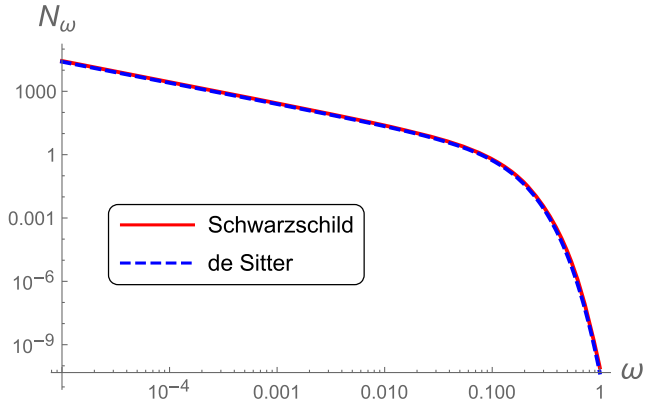

FIG. 4. The particle count spectra $N_\omega = \int N_{\omega\omega'} d\omega'$. Blue and red curves are the same, showing that both de Sitter and late-time Schwarzschild solutions have thermal spectra at temperature $\kappa/2\pi$. Here we have chosen $\kappa = 1/4$ for illustration.

function divergence (see also e.g., [32]) can be removed easily by using finite normalization wave packet modes [4]. The de Sitter calculation is not as straightforward as the Schwarzschild black hole and is therefore outlined in Appendix C.

Surprisingly, despite infinite acceleration and constant energy flux, Eq. (20), for all times u, the two horizons in v appear to conspire to render the total emitted energy,

$$E = \int_0^\infty d\omega \omega N_\omega = \text{finite}, \quad (26)$$

finite. The closed form result for E is challenging analytically, but straightforward numerically. Computing Eq. (26) for $\kappa = 1$ gives $E \approx 5$. Equation (26) is the energy carried by the particles and contrasts with the energy of radiation,

$$E = \int_{-\infty}^\infty du F(u) = \text{infinite}, \quad (27)$$

resulting from the quantum stress tensor measured at $\mathcal{I}^+_R$. A similar finite energy to Eq. (26) is obtained using a finite-lifetime mirror in [28]. Following Eq. (23), we plot $E_{\omega\omega'} = \omega N_{\omega\omega'}$ in Fig. 5.

IV. FROM DE SITTER TO ANTI-DE SITTER

Reference [33] showed that constant thermal flux had a simple condition when written in terms of proper time (see Appendix B 1) and identified three forms for the moving mirror acceleration satisfying this. The first solution is the Carlitz-Willey mirror and the second is the de Sitter mirror, the focus of this article. The third solution gives the mirror corresponding to anti-de Sitter (AdS) spacetime. This eternally gives off negative energy flux, $F = -\kappa^2/(48\pi)$.

For AdS $f_L = 1 + r^2/L^2$, which can be thought of as $L^2 = 1/\Lambda$ being negative. AdS space does not have a horizon, but does have an edge at the origin $r = 0$ with the

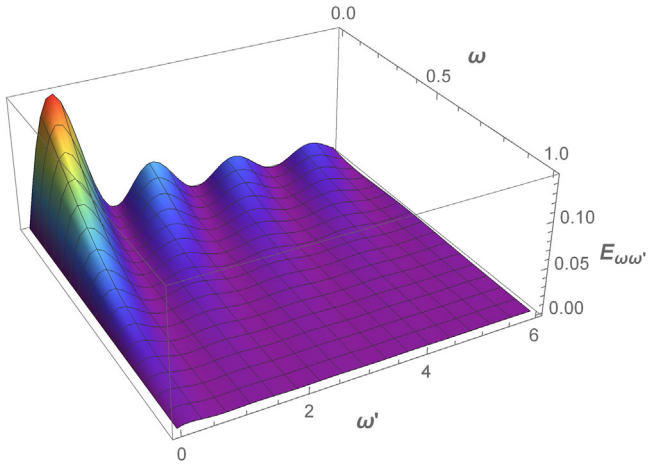

FIG. 5. The total energy carried by the particles, Eq. (26), emitted by the de Sitter mirror is finite. The integrand $E_{\omega\omega'}$ exhibits dips in energy as seen in $N_{\omega\omega'}$ from Fig. 3. There is no infrared divergence, as the limit of $E_{\omega\omega'}$ when $\omega \to 0$ is $\sin^2(2\omega')/(\pi^2\omega')$.

same regularity requirement as the de Sitter accelerated boundary correspondence (ABC). Taking the de Sitter κ imaginary turns tanh into tan, so

$$f(v) = \frac{2}{\kappa^*}\tan^{-1}\frac{\kappa^* v}{2}. \tag{28}$$

This trajectory is the ABC of the AdS spacetime. The nonzero beta coefficients are given, by symmetry, through $\beta^{dS}_{\omega\omega'} = -\beta^{\mathrm{AdS}}_{\omega'\omega}$. While many mirrors incite episodes of negative energy flux (and indeed unitarity requires it for asymptotically static mirrors [34]), here the total energy is negative. Since the relationships between particles and energy in quantum field theory are far from resolved, this trajectory provides a good illustration of the pressing issues raised in association with negative energy radiation carried by nontrivial particle production processes.

V. CONCLUSIONS

We have solved for the particle spectrum associated with de Sitter cosmology for the de Sitter moving mirror. This is the second of the eternal thermal mirrors (with the first being the Carlitz-Willey solution for Schwarzschild spacetime, and the third, also presented here, corresponding to anti-de Sitter cosmology).

The beta Bogoliubov coefficients can be written in terms of special functions, and give rise to a particle spectrum with a Planck distribution with temperature inversely proportional to the horizon scale (or proportional to the square root of the cosmological constant).

The solution has some interesting properties: isolated zeros in the particle count per mode squared despite a thermal particle count spectrum, which may be related to destructive interference between the double horizons, and finite total energy emission derived via quantum summing, and numerically verified, which contrasts with the infinite energy via an eternally thermal quantum stress tensor.

Despite the ambiguities in the convergence of the total energy emission and interpretation of the zeros in $|\beta_{\omega\omega'}|^2$, and though this calculation has been done for a simple $(1+1)$-dimensional model, we believe the results increase one's understanding of the particle production of de Sitter cosmology identified with this moving mirror. As the completion of the trio of eternal thermal mirrors, the results show the connections and differences with the Carlitz-Willey solution for Schwarzschild spacetime.

The accelerated boundary correspondence (ABC) is demonstrated to be a useful tool, enabling us to use the derived de Sitter moving mirror solution to confirm that the distribution of particles produced from a massless scalar quantum field is the thermal Planck spectrum, with temperature related to the horizon scale, or alternately mirror acceleration.

ACKNOWLEDGMENTS

M. G. thanks Joshua Foo and Daiqin Su for stimulating and helpful correspondence. Funding from state-targeted program "Center of Excellence for Fundamental and Applied Physics" (BR05236454) by the Ministry of Education and Science of the Republic of Kazakhstan is acknowledged. M. G. is also funded by the ORAU FY2018-SGP-1-STMM Faculty Development Competitive Research Grant No. 090118FD5350 at Nazarbayev University. E. L. is supported in part by the Energetic Cosmos Laboratory and by the U.S. Department of Energy, Office of Science, Office of High Energy Physics, under Award No. DE-SC-0007867 and Contract No. DE-AC02-05CH11231.

APPENDIX A: EUCLIDEAN METHOD

Gibbons-Hawking [5] showed that thermal radiation emanates from the de Sitter horizon, similar to the radiation emanating from the Schwarzschild black hole horizon [4] and to the radiation seen by an accelerated observer in the Unruh effect [15]. Dimensional analysis of the system immediately gives $T \sim 1/L$, while the proportionality factor of 2π can be obtained via Wick rotation. The static patch has a Euclidean continuation by taking $t_E = it$, resulting in

$$ds^2 = +f_L dt_E^2 + f_L^{-1} dr^2 + r^2 d\Omega. \tag{A1}$$

The periodicity of Euclidean time, with period $\beta = 2\pi L$ implies a temperature $T = (2\pi L)^{-1}$. Essentially, de Sitter space can be viewed as a finite cavity surrounding the observer, with the horizon as its boundary [7].

APPENDIX B: PROPER, RETARDED AND ADVANCED TIME DYNAMICS

1. Proper time

The second of the constant thermal flux solutions in [33] had the proper acceleration written in proper time as

$$\alpha(\tau) = -\frac{\kappa}{2}\tan\frac{\kappa\tau}{2}. \tag{B1}$$

The rapidity being its integral, $\alpha = d\eta/d\tau$,

$$\eta(\tau) = \ln\cos\frac{\kappa\tau}{2}. \tag{B2}$$

The celerity (proper velocity) is $w = \sinh\eta$,

$$w(\tau) = -\csc(\kappa\tau)\sin^3\frac{\kappa\tau}{2}. \tag{B3}$$

The Lorentz factor $\gamma = \cosh\eta$ is

$$\gamma(\tau) = \frac{1}{4}(\cos(\kappa\tau)+3)\ \sec\frac{\kappa\tau}{2}. \tag{B4}$$

Conversion can be done between $u \leftrightarrow \tau$, via $e^{\eta} = d\tau/du$ integration,

$$\tanh\frac{\kappa u}{4} = \tan\frac{\kappa\tau}{4}. \tag{B5}$$

While tan ranges from $-\infty$ to $+\infty$ and tanh ranges -1 to 1, the periodicity of the system is manifest, when $\kappa\tau = -\pi$ or argument $n\pi/2$ odd integer values thereof. This is also apparent in the zero denominator of

$$\tanh\frac{\kappa u}{4} = \frac{1+\sin(\kappa\tau/2)-\cos(\kappa\tau/2)}{1+\sin(\kappa\tau/2)+\cos(\kappa\tau/2)}, \tag{B6}$$

at the same locations. The trajectory is checked via $w = dx/d\tau$,

$$x(\tau) = \frac{1}{\kappa}\sin\frac{\kappa\tau}{2} + \frac{1}{\kappa}\ln\left(\frac{2}{\tan\frac{\kappa\tau}{4}+1}-1\right), \tag{B7}$$

or in delayed time u via Eq. (B6),

$$x(u) = \frac{1}{\kappa}\tanh\frac{\kappa u}{2} - \frac{u}{2}, \tag{B8}$$

which gives the inverse of $f(v) = p^{-1}(u)$, Eq. (15), or just simply Eq. (B11),

$$v = p(u) = \frac{2}{\kappa}\tanh\frac{\kappa u}{2}. \tag{B9}$$

An advantage of proper time is that the derivation of constant energy flux is particularly simple:

$$F(\tau) = -\frac{1}{12\pi}\eta''(\tau)e^{2\eta(\tau)} = \frac{\kappa^2}{48\pi}, \tag{B10}$$

agreeing with Eq. (20).

2. Retarded time

In delayed or retarded time u, the flux is $-24\pi F(u) = \{p(u), u\}$, where $p(u)$ is Eq. (B11), giving Eq. (20), $F = \kappa^2/(48\pi)$. The trajectory in light cone coordinates as a function of retarded time $u = t - x$ is $f(v) = p^{-1}(u)$,

$$p(u) = \frac{2}{\kappa}\tanh\frac{\kappa u}{2}. \tag{B11}$$

The rapidity,

$$\eta(u) = \ln\operatorname{sech}\frac{\kappa u}{2}, \tag{B12}$$

can be used to find the acceleration via

$$\alpha(u) = e^{-\eta(u)}\eta'(u), \tag{B13}$$

which gives

$$\alpha(u) = -\frac{\kappa}{2}\sinh\frac{\kappa u}{2}. \tag{B14}$$

Retarded time u is convenient because it is the time of the observer at $\mathcal{I}_R^+$ but the integration for the beta coefficients is not tractable. The beta coefficients are however, tractable using advanced time v.

3. Advanced time

In advanced time $v = t + x$ the flux is in the form of Eq. (18) which results in Eq. (20). The proper acceleration is obtained through the conversion from τ to v. Starting with

$$\frac{dv}{d\tau} = \frac{d(t+x)}{d\tau} = \cosh\eta + \sinh\eta \tag{B15}$$

and using once again $\alpha = d\eta/d\tau$, so η becomes

$$\eta = \ln\cos\frac{\kappa\tau}{2}, \tag{B16}$$

after integration we find

$$v = \frac{2}{\kappa}\sin\frac{\kappa\tau}{2}. \tag{B17}$$

Expressing τ and inserting it into Eq. (B1) we get the proper acceleration in terms of advanced time,

$$\alpha(v) = -\frac{1}{2}\frac{\kappa^2 v}{\sqrt{4-\kappa^2 v^2}}, \tag{B18}$$

precisely Eq. (17). Thus the second eternal thermal flux solution of [33] is indeed equivalent to the de Sitter case.

APPENDIX C: EXPLICIT CALCULATION OF THE PLANCK SPECTRA FOR DE SITTER'S MOVING MIRROR

Thermal behavior is seen by the expectation value:

$$\mathcal{N}_\omega \equiv \int_0^{+\infty} d\omega' \beta_{\omega\omega'}\beta^*_{\omega_2\omega'} = \frac{\delta(\omega-\omega_2)}{e^{2\pi\omega/\kappa}-1}. \tag{C1}$$

We derive this starting with the beta coefficients. After an integration by parts, we have

$$\beta_{\omega\omega'} = \frac{2\omega'}{4\pi\sqrt{\omega\omega'}}\int_{-2/\kappa}^{+2/\kappa} dv_1 V_1^{-i\omega/\kappa} e^{-i\omega' v_1}, \tag{C2}$$

and its complex conjugate counterpart,

$$\beta^*_{\omega_2\omega'} = \frac{2\omega'}{4\pi\sqrt{\omega_2\omega'}}\int_{-2/\kappa}^{+2/\kappa} dv_2 V_2^{i\omega_2/\kappa} e^{i\omega' v_2}, \tag{C3}$$

where $V_i \equiv (1+\kappa v_i/2)/(1-\kappa v_i/2)$. The spectrum $\mathcal{N}_\omega$ scales as

$$\mathcal{N}_\omega \sim \int d\omega' \int dv_1 \int dv_2 V_1^{-i\omega/\kappa} V_2^{i\omega_2/\kappa} \omega' e^{-i\omega'(v_1-v_2)}, \tag{C4}$$

where the proportionality factor is $1/(4\pi^2\sqrt{\omega\omega_2})$. The ω' integration is done via the introduction of a real $\epsilon > 0$ regulator,

$$\int_0^\infty d\omega' \omega' e^{-i\omega' Z} = -\frac{1}{(Z-i\epsilon)^2}, \tag{C5}$$

giving

$$\mathcal{N}_\omega = \frac{-1}{4\pi^2\sqrt{\omega\omega_2}}\int dv_1 \int dv_2 \frac{V_1^{-i\omega/\kappa} V_2^{i\omega_2/\kappa}}{(v_1-v_2-i\epsilon)^2}. \tag{C6}$$

A substitution via variables $v_i = (2/\kappa)\tanh 2S_i$ results in

$$\mathcal{N}_\omega = \frac{-1}{4\pi^2\sqrt{\omega\omega_2}}\int dS_1 \int dS_2 \frac{4e^{-4i(\omega S_1 - \omega_2 S_2)/\kappa}}{\sinh^2(2(S_1-S_2))}, \tag{C7}$$

to leading order in small ϵ. A second substitution simplifies via $Q_{p,m} \equiv S_1 \pm S_2$ to

$$\mathcal{N}_\omega = \frac{-1}{2\pi^2\sqrt{\omega\omega_2}}\int dQ_p e^{-2i\omega_m Q_p/\kappa}\int dQ_m \frac{e^{-2i\omega_p Q_m/\kappa}}{\sinh^2(2Q_m - i\epsilon)}, \tag{C8}$$

where $\omega_{p,m} \equiv \omega \pm \omega_2$, and a new ϵ has been introduced, and a Jacobian of $1/2$. The first integral is the Dirac delta, so

$$\mathcal{N}_\omega = \frac{2\pi(\kappa/2)\delta(\omega_m)}{2\pi^2\sqrt{\omega\omega_2}}\int dQ_m \frac{-e^{-2i\omega_p Q_m/\kappa}}{\sinh^2(2Q_m - i\epsilon)}. \tag{C9}$$

We can drop the subscript now, $Q_m := Q$. For the next integral, we will use the identity

$$\frac{1}{\sinh^2(\pi x)} = \sum_{k=-\infty}^{+\infty}\frac{1}{(\pi x + i\pi k)^2}, \tag{C10}$$

and now $\omega_p = 2\omega$, to write

$$\frac{-e^{-2i\omega_p Q/\kappa}}{\sinh^2(2Q-i\epsilon)} = \sum_{k=-\infty}^{+\infty}\frac{-e^{-4i\omega Q/\kappa}}{(2Q - i\epsilon + i\pi k)^2}. \tag{C11}$$

First integrating,

$$\sum_{k=-\infty}^{+\infty}\int_{-\infty}^{+\infty} dQ \frac{-e^{-4i\omega Q/\kappa}}{(2Q-i\epsilon+i\pi k)^2} = \frac{2\pi\omega}{\kappa}\sum_{k=1}^{+\infty} e^{-2\pi k\omega/\kappa}, \tag{C12}$$

so that

$$\mathcal{N}_\omega = \delta(\omega_m)\sum_{k=1}^{+\infty} e^{-2\pi k\omega/\kappa}, \tag{C13}$$

we then sum, giving the final result:

$$\mathcal{N}_\omega = \frac{\delta(\omega-\omega_2)}{e^{2\pi\omega/\kappa}-1}. \tag{C14}$$

We can compare to the Schwarzschild mirror [35], which has beta coefficient squared

$$N^S_{\omega\omega'} := |\beta^S_{\omega\omega'}|^2 = \frac{\omega'}{2\pi\kappa(e^{2\pi\omega/\kappa}-1)(\omega'+\omega)^2}, \tag{C15}$$

with $\kappa = 1/(4M)$. In the high frequency regime, where the modes are extremely redshifted, $\omega' \gg \omega$, one has the per mode squared spectrum $N_{\omega\omega'} := |\beta_{\omega\omega'}|^2$ (not N_ω) as

$$N^S_{\omega\omega'} = \frac{1}{2\pi\kappa\omega'}\frac{1}{e^{\omega/T_s}-1}, \tag{C16}$$

where the Schwarzschild temperature is $T_s = \kappa/(2\pi)$. The de Sitter result is eternally thermal, while the collapse to the Schwarzschild black hole is only late-time thermal. The Schwarzschild result for $\mathcal{N}^S_\omega$ proceeds [17] to the penultimate result

$$\mathcal{N}^S_\omega = \frac{\kappa}{2\pi\omega}\left|\Gamma\left(1+i\frac{\omega}{\kappa}\right)\right|^2 e^{-\pi\omega/\kappa}\delta(\omega_m), \tag{C17}$$

which reduces to $\mathcal{N}^S_\omega = \delta(\omega_m)(e^{2\pi\omega/\kappa}-1)^{-1}$, identical in form to Eq. (C14).

[1] E. Schrödinger, Physica (Amsterdam) **6**, 899 (1939).
[2] G. T. Moore, J. Math. Phys. (N.Y.) **11**, 2679 (1970).
[3] P. Davies, S. Fulling, and W. Unruh, Phys. Rev. D **13**, 2720 (1976).
[4] S. W. Hawking, Commun. Math. Phys. **43**, 199 (1975).
[5] G. W. Gibbons and S. W. Hawking, Phys. Rev. D **15**, 2738 (1977).
[6] M. Spradlin, A. Strominger, and A. Volovich, in *Les Houches Summer School: Session 76: Euro Summer School on Unity of Fundamental Physics: Gravity, Gauge Theory and Strings* (2001), pp. 423–453 [arXiv:hep-th/0110007].
[7] V. Balasubramanian, P. Horava, and D. Minic, J. High Energy Phys. 05 (2001) 043.
[8] A. D. Linde, Lect. Notes Phys. **738**, 1 (2008).
[9] S. A. Fulling and P. C. W. Davies, Proc. R. Soc. A **348**, 393 (1976).
[10] P. Davies and S. Fulling, Proc. R. Soc. A **356**, 237 (1977).
[11] P. Chen and G. Mourou, arXiv:2004.10615.
[12] P. Chen and G. Mourou, Phys. Rev. Lett. **118**, 045001 (2017).
[13] P. Davies, J. Phys. A **8**, 609 (1975).
[14] S. Fulling and J. Wilson, Phys. Scr. **94**, 014004 (2019).
[15] W. G. Unruh, Phys. Rev. D **14**, 870 (1976).
[16] F. Wilczek, in *International Symposium on Black holes, Membranes, Wormholes and Superstrings* (1993), pp. 1–21 [arXiv:hep-th/9302096].
[17] A. Fabbri and J. Navarro-Salas, *Modeling Black Hole Evaporation* (Imperial College Press, London, 2005).
[18] N. G. Sanchez, Phys. Lett. B **87**, 212 (1979).
[19] N. G. Sanchez, Phys. Lett. B **105**, 375 (1981).
[20] N. Birrell and P. Davies, *Quantum Fields in Curved Space*, Cambridge Monographs on Mathematical Physics (Cambridge University Press, Cambridge, England, 1984).
[21] M. R. R. Good and Y. C. Ong, J. High Energy Phys. 07 (2015) 145.
[22] M. R. R. Good, in *2nd LeCosPA Symposium: Everything about Gravity, Celebrating the Centenary of Einstein's General Relativity* (2017), pp. 560–565 [arXiv:1602.00683].
[23] P. R. Anderson, M. R. R. Good, and C. R. Evans, in *The Fourteenth Marcel Grossmann Meeting* (2017), pp. 1701–1704 [arXiv:1507.03489].
[24] M. R. R. Good, P. R. Anderson, and C. R. Evans, in *The Fourteenth Marcel Grossmann Meeting* (2017), pp. 1705–1708 [arXiv:1507.05048].
[25] M. R. Good, Phys. Rev. D **101**, 104050 (2020).
[26] M. R. R. Good and Y. C. Ong, arXiv:2004.03916.
[27] M. R. R. Good, K. Yelshibekov, and Y. C. Ong, J. High Energy Phys. 03 (2017) 013.
[28] J. Foo, S. Onoe, M. Zych, and T. C. Ralph, arXiv:2004.07094.
[29] D. Su and T. C. Ralph, Phys. Rev. D **93**, 044023 (2016).
[30] P. Martinetti and C. Rovelli, Classical Quantum Gravity **20**, 4919 (2003).
[31] R. D. Carlitz and R. S. Willey, Phys. Rev. D **36**, 2327 (1987).
[32] M. Horibe, Prog. Theor. Phys. **61**, 661 (1979).
[33] M. R. Good and E. V. Linder, Phys. Rev. D **97**, 065006 (2018).
[34] M. R. Good, E. V. Linder, and F. Wilczek, Phys. Rev. D **101**, 025012 (2020).
[35] M. R. Good, P. R. Anderson, and C. R. Evans, Phys. Rev. D **94**, 065010 (2016).